

ANALYSIS OF LAND USE DATA AND SURFACE TEMPERATURES DERIVED FROM SATELLITE DATA FOR THE AREA OF BERLIN

Kerstin MUNIER, Heinz BURGER

Freie Universität Berlin, Institut für Geologische Wissenschaften,
Fachrichtung Geoinformatik
Malteserstrasse 74-100, 12249 Berlin, Germany

ABSTRACT

Surface temperatures derived from Landsat 5 and Landsat 7 data were analysed for a late-summer day in 1991 and a midsummer day in 2000. For both dates a scene from a night pass and a scene from the day pass of the following morning were processed and compared. The daytime surface temperatures, the night-time surface temperatures and the differences between night and day were linked to data about the land use within the city of Berlin for further investigations of the relationship between temperature behaviour and urban structures. The Normalised Difference Vegetation Index (NDVI) was used to examine the relation between thermal behaviour and vegetation cover amount. Water and forest cover types show low day-night temperature differences compared to residential, commercial and agricultural cover types.

1 INTRODUCTION

Surface temperature is the basic parameter for the deviation of the thermal behaviour of the environment. The main objective of this paper is to apply Landsat TM thermal imagery to analyse the change of surface temperature in Berlin using two day-night pairs of Landsat TM acquired in 1991 and 2000. About 23,000 polygons containing land use cover types and urban structure types were provided by the municipal administration. The thermal bands of the satellite images were transformed into surface temperature values and these layers were intersected with land use cover polygons. Multivariate statistical methods were applied to analyse

- temperature differences between each day- and night-time pair (1991, 2000)
- the change of these differences from 1999 to 2000, and
- cooling characteristics for different land-cover types.

2 STUDY AREA

Berlin is the capital and the biggest city of Germany. It has about 3.5 million inhabitants living in an area of 889 square kilometres. Berlin has been undergoing a rapid transformation since the reunification of both parts of Germany on October 3, 1990. This is the most important change since 1920, when 7 nearby towns and about 60 villages around the historical core of the city were merged to form one municipality called "Greater Berlin" and the consequences of World War II. This agglomerative structure is still visible on satellite images. The dominating cover types and conspicuous features on satellite images of the city of Berlin are:

1. the historical centre of Berlin, a rapidly changing business district adjoining a large urban recreation park, the Tiergarten
2. urban cores around this centre, characterised by high building density
3. chains of lakes connected by rivers or canals. Many industrial areas border these waterways
4. large urban forest areas in the west and south-east of Berlin
5. two airports (Tempelhof and Tegel) within the city area.

3 DATA PROCESSING

In 1991 a pair of day-night-time Landsat 5 TM scenes of Berlin and its surroundings was analysed with respect to surface temperature.

Night-time scene Path 49 Row 222 from Sept. 14th 1991; about 21.45 CET
 Daytime scene Path 193 Row 23 from Sept. 15th 1991; about 10.45 CET

Maps of these results were published in the Environmental Atlas of Berlin (1995). In order to update these results a new pair of day-night-time scenes was ordered, now Landsat 7 ETM+ with different sensor parameters. A list of sensor parameters for both systems is given in Table 1.

	Landsat 5 TM		Landsat 7 ETM+	
	spectral	spatial resolution	spectral	spatial resolution
Band 1	0.45-0.52 μm	30 m	0.450-0.515 μm	30 m
Band 2	0.52-0.60 μm	30 m	0.525-0.605 μm	30 m
Band 3	0.63-0.69 μm	30 m	0.630-0.690 μm	30 m
Band 4	0.76-0.90 μm	30 m	0.775-0.900 μm	30 m
Band 5	1.55-1.75 μm	30 m	1.550-1.750 μm	30 m
Band 6 / 6.1	10.40-12.50 μm	120 m	10.40-12.50 μm	60 m
Band 6.2	-	-	10.40-12.50 μm	60 m
Band 7	2.08-2.35 μm	30 m	2.090-2.350 μm	30 m
Band 8	-	-	0.520-0.900 μm	15 m

Table 1: Spectral and spatial resolution of the actual Landsat sensors

The weather condition from Aug. 14th to 15th were very good: no cloud cover, slight dust in the atmosphere.

Night-time scene Path 49 Row 222 from Aug. 13th 2000; about 21.45 CET
 Daytime scene Path 193 Row 23 from Aug. 14th 2000; about 10.45 CET

This date – one month earlier than the 1991 scenes - is not optimal for a comparative study, but it was the only chance for this type of data acquisition during summertime in 2000.

3.1 GEOMETRIC CORRECTION

Geometric image correction was performed using corresponding ground control points in the GIS layer and the panchromatic band of the Landsat image which has best spatial resolution. Bilinear resampling was applied in order to preserve linear features. The RMS-error is < 1 related to a $15 \times 15 \text{ m}^2$ pixel size. The geometrically corrected panchromatic image was used as "master" for the geometric correction of all other data sets (multi-spectral bands incl. thermal bands of day- and night-time scenes of 1991 and 2000).

3.2 CALCULATION OF RADIANCE TEMPERATURE

The digital numbers were transformed into absolute radiance (see: SCHOTT & VOLCHOCK, 1985; <http://ltpwww.gsfc.nasa.gov/IAS/handbook>) using

$$L_{\lambda} = (L_{\max} - L_{\min})/255 * \text{DN} + L_{\min} \quad (1)$$

where L_{λ} is the spectral radiance, L_{\min} and L_{\max} [$\text{mW cm}^{-2} \text{sr}^{-1} \mu\text{m}^{-1}$] are spectral radiances for each band at digital numbers 0 and 255 respectively. For TM 5 L_{\min} and L_{\max} the values 0.124 and 1.560 [$\text{mW cm}^{-2} \text{sr}^{-1} \mu\text{m}^{-1}$] resp. were taken from the literature. For the new sensors in TM 7 the following reference values are given:

ETM+ Spectral Radiance Range:

Low Gain: L_{\min} - 0.0 L_{\max} - 17.04 watts/(meter squared * ster * μm)
 High Gain: L_{\min} - 3.2 L_{\max} - 12.65 watts/(meter squared * ster * μm)

The spectral radiances L_{λ} were converted into effective at-satellite temperatures T by

$$T = K2 / \ln (K1 / L_{\lambda} + 1) \quad (2)$$

where $K1$, $K2$ are calibration constants. For Landsat 5 TM the constants $K1 = 60,776 \text{ mW} \cdot \text{cm}^{-2} \cdot \text{sr}^{-1} \cdot \mu\text{m}^{-1}$ and $K2 = 1260,56 \text{ K}$ were taken; for Landsat ETM+ the NASA-handbook gives $K1 = 666,09 \text{ w} \cdot \text{m}^{-2} \cdot \text{sr}^{-1} \cdot \mu\text{m}^{-1}$ and $K2 = 1282,71 \text{ K}$ respectively. For Landsat ETM+ the values were also given in the header information of the thermal bands.

The resulted temperature represents an “effective at-satellite temperature of the viewed Earth-atmosphere system under the assumption of unity emissivity” (<http://tpwww.gsfc.nasa.gov/IAS/handbook>). The consideration of emissivity of the surface cover types would include the additional problem of mixed pixels in a $60 \times 60 \text{ m}^2$ area. Otherwise the mixed signatures help to accept the assumption of unity emissivity for this kind of application. No atmospheric correction was carried out for this comparative study. In this way the term surface temperature is not correct but should describe the representation of the thermal behaviour of surface cover types under these discussed conditions. The temperatures are also not directly comparable with air temperatures normally measured 2 meters above ground. Simultaneous measurements of temperature of water bodies directly at surface 1991 and 2000 correspond with the calculated temperature in a range of 1 Kelvin by an emissivity of water of about 0.98 – 0.99.

Temperatures were converted from degree Kelvin into degree Celsius for simpler handling. After calculation of day-night differences and the changes of day-night differences between 1991 and 2000 the values were rounded to 1° K resp. 1° Celsius in order to create larger homogeneous areas which can be converted from raster into vector format with a number of polygons which is manageable for GIS operations.

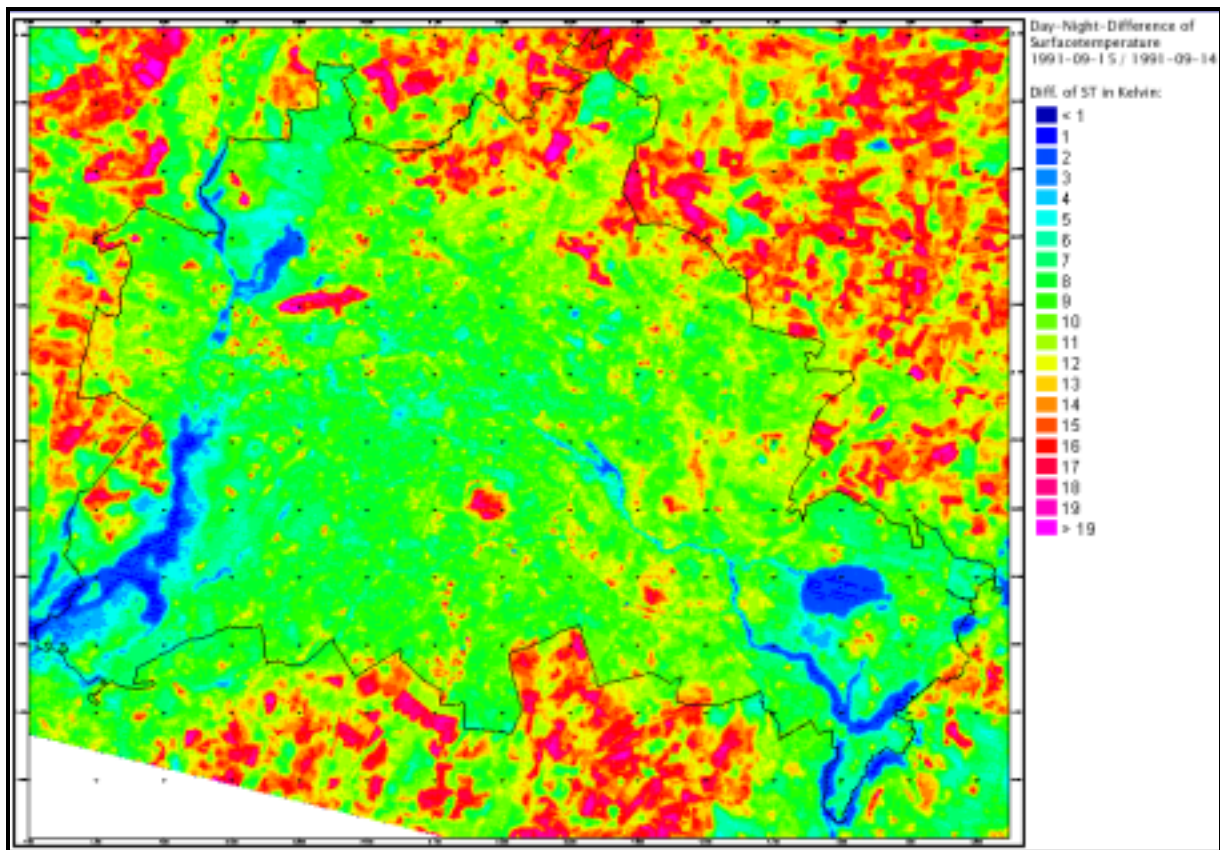


Fig. 1: Differences of surface temperature of Berlin for the scene pair of 1991

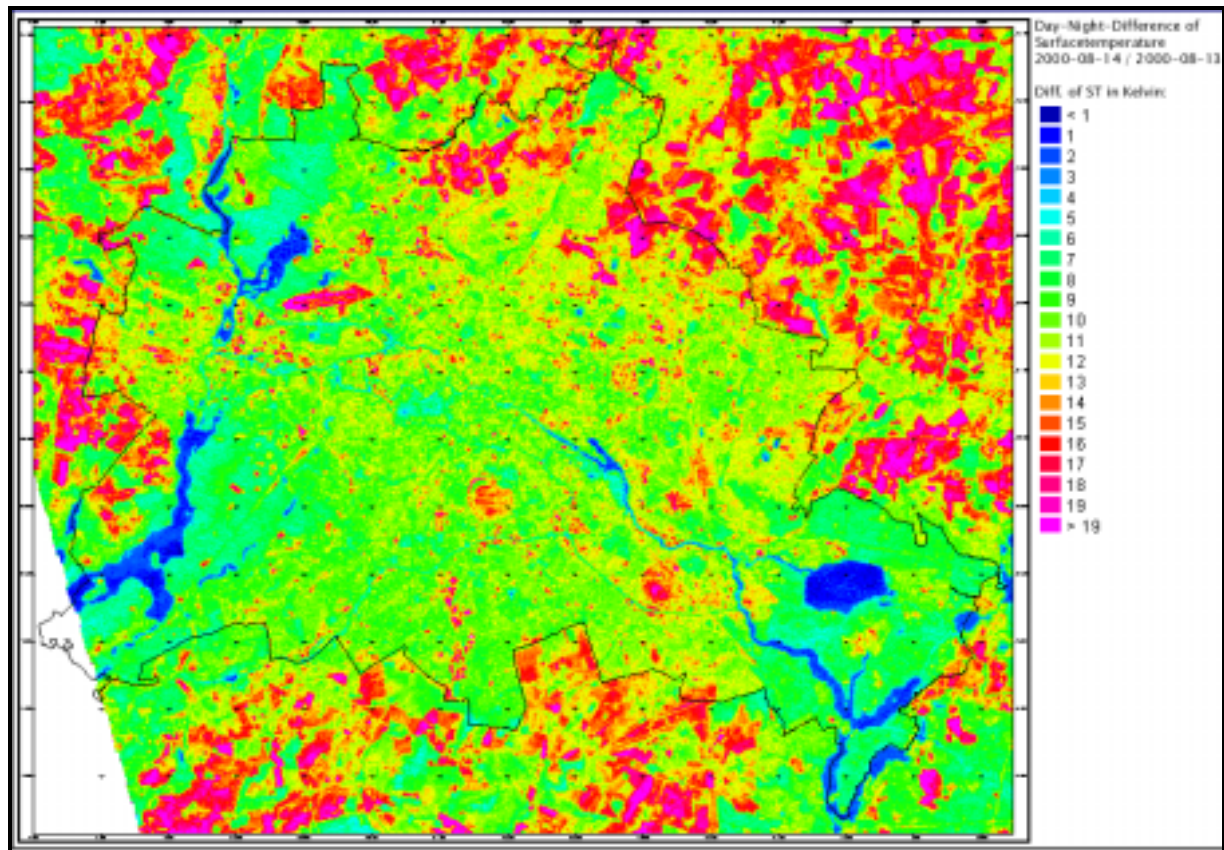


Fig. 2: Differences of surface temperature of Berlin for the scene pair of 2000

3.3 RELATION BETWEEN LAND COVER TYPES AND SURFACE TEMPERATURE

The polygon layer contains about 23,000 polygons and includes thematic information about polygon area, proportion of sealed area (in %), land-cover type, and urban structure type. The intersection of this polygon layer with temperature layers for daytime and night-time surface temperatures as well as day-night-time temperature differences produced up to 316,000 polygons containing information from both layers. For each land-cover polygon was calculated the mean temperature weighted by the area of each contributing intersection polygon. The results were stored in a data base which is the basis for all statistical analyses and spatial visualisations.

4 ANALYSIS

A map of surface temperatures for Berlin derived from Landsat 5 satellite imagery was published in the Environmental Atlas of Berlin. It was the main goal of the municipal customer (Senate Department for Urban Development) to compare this map with recent data obtained by Landsat 7 and to validate the polygon layer of the urban structures which will be a basis for urban planning. The data base contains ca. 100 urban structure types (e.g. post office, university, hospital, school etc.) and 30 land use cover types. For remote sensing applications only the land use cover types are meaningful (see Table 2).

Index	L_U_KEY	land use
10	res	residential general (housing share dominant)
21	res1	residential mix1 (interspersed commercial enterprises)
22	res2	residential mix2 (high share of production
23	res3	residential mix (former East Berlin)
30	resKern	residential core with high density
40	c&i	commercial and industrial enterprises
50	se1	service (public facilities: universities, schools, playgrounds)
60	se2	service (utility areas: power plants, public transportation)
70	ve_ag1	allotment gardens
80	se_traff	traffic areas
90	b_site	building site
100	for_gen	forest general
101	for_int	forest internal
102	for_ext	forest external
110	water	water bodies
121	ve_green	green spaces (meadows, pastures)
122	fields2	fields (farmland, periodically sown and harvested)
130	ve_park	parks
140	se_prom	promenades & city squares
150	ve_cem	cemetery
160	ve_ag2	allotment gardens
161	ve_ag3	allotment gardens < 10% permanent residents
162	ve_ag4	allotment gardens > 10% permanent residents
171	fields1	fields (bare soils, vacant areas)
172	ve_mead	meadows
173	ve_mix	mixed vegetation
174	for_mix	mixed forest
180	camp	campsite
190	se_sport	sports fields
200	ve_nurs	tree nursery/horticulture

Table 2: Land use/cover key for Berlin

This list contains a combination of built-up area classification and greenland inventory. Some of these categories are overlapping and some categories are difficult to delimitate. This hold especially for the various types of allotment gardens and colonies, which are (still) typical for Berlin (for a detailed description of these categories see <http://www.stadtentwicklung.berlin.de/umwelt/umweltatlas/>).

4.1 COMPARISON OF SURFACE TEMPERATURE IN 1991 AND 2000

The statistical analysis of the mean surface temperature (MST) for all land cover types shows a strong correlation ($r=0.89$) between the daytime MST in 1991 and 2000 as well as for the night-time pair ($r=0.83$, see Table 3). There is no correlation between day-night temperatures. This result confirms that the night path of Landsat TM provides independent information about the thermal behaviour of the earth surface – a fact which is still under-utilised in remote sensing studies. Table 3 also contains correlation coefficients for sealing density VG and normalised difference vegetation indices NDVI (see Chap. 4.3).

	D91MT	D00MT	N91MT	N00MT	DIF91MT	DIF00MT	NDVI91	NDVI00	DD00M91	VG
D91MT	1.00	0.89	-0.02	0.05	0.75	0.81	-0.69	-0.67	0.21	0.48
D00MT	0.89	1.00	0.03	0.12	0.63	0.87	-0.70	-0.73	0.52	0.56
N91MT	-0.02	0.03	1.00	0.83	-0.67	-0.37	-0.38	-0.35	0.48	0.41
N00MT	0.05	0.12	0.83	1.00	-0.52	-0.36	-0.42	-0.42	0.23	0.44
DIF91MT	0.75	0.63	-0.67	-0.52	1.00	0.84	-0.25	-0.25	-0.17	0.07
DIF00MT	0.81	0.87	-0.37	-0.36	0.84	1.00	-0.46	-0.49	0.39	0.31
NDVI91	-0.69	-0.70	-0.38	-0.42	-0.25	-0.46	1.00	0.92	-0.42	-0.72
NDVI00	-0.67	-0.73	-0.35	-0.42	-0.25	-0.49	0.92	1.00	-0.46	-0.72
DD00M91	0.21	0.52	0.48	0.23	-0.17	0.39	-0.42	-0.46	1.00	0.45
VG	0.48	0.56	0.41	0.44	0.07	0.31	-0.72	-0.72	0.45	1.00

Tab. 3: Correlation matrix for MST for all land use cover types. D91MT, D00MT: daytime temperatures; N91MT, N00MT: night temperatures; DIF91, DIF00: day-night differences; DD00M91: DIF00 minus DIF91; NDVI91, NDVI00: normalised difference vegetation indices; VG: sealing density (from land cover layer)

Average STs for all land cover types are listed in Table 4. During the daytime commercial/industrial areas as well as certain agricultural and residential cover types exhibit the highest STs, forest and water the lowest. More important for the urban climate are day-night ST-differences. It is well known that agricultural land use areas exhibit the highest day-night temperature contrast, residential areas, industrial and commercial cover types show mid-range contrast values, water and forest cover the lowest contrast. Fig. 1 + 2 show day-night ST contrast images for Berlin and its surroundings in 1991 and 2000 (area 46 km x 38 km). High ST contrast (yellow/red colours) dominate the rural environment outside the border of Berlin (black line) and both city airports; lakes and adjacent forest areas in the west and south east are characterised by low ST contrast (blue/green colours). The global mean temperature difference for the 2000 scene pair is ca. 1° C higher than in 1991 which may be explained by different weather conditions in 1991 and 2000 (see last line in Table 4) or different sensor characteristics for Landsat 5 TM and Landsat 7 ETM+.

Cluster analysis based on average day-night surface temperatures for all 30 land cover types was applied in order to create new groups based on their thermal properties. A dendrogram and scattergrams of day-night MST (year 2000) for all land cover types are given in App. 1. If the dendrogram (App. 1a) is cut at a level of 5 clusters (rescaled distance: 5) we obtain the following **5 groups** with similar thermal characteristics:

1. Forest cover and water bodies
2. Grassland (meadows, pastures)
3. Areas with a mixture of trees, meadows, residential use
4. All other residential/commercial and service areas (subdivided into 4a, 4b)
5. Bare soil/vacant areas (fields2)

The scattergram of MSTs (App. 1b) and a factor analysis based on both day/night MST values confirm this clustering result, but there is a continuous transition from one group to the other (see scattergram of factor scores in App. 1c).

The main problem of change detection based on MST for urban blocks is the insensitivity of this parameter due to the high variability within each urban structure type and within each polygon. This becomes obvious if we look at a more detailed image of MST related to the urban structure polygons at **Potsdamer Platz**: Fig. 3 + 4 show the block structure, mean surface temperatures, differences and mean NDVI values extracted from ETM+ (area 3 km x 3.6 km). The variability for all variables is rather high for small polygons and we can assume that the internal structure of large polygons is not as homogeneous as the GIS-database indicates. The big range of polygon sizes will influence the sensitivity for land use changes: if only small areas are affected by land cover changes then the MST will differ significantly only in small urban structure polygons. This effect is demonstrated in Fig. 5 + 6 where MST for blocks and temperature information for pixels is displayed. After the reunification of both parts of Berlin Potsdamer Platz was one of the biggest construction sites in Europe. In this case the MST for rather big urban structure polygons exhibits significant changes. The situation is different for an industrial area in the north of Berlin. Here we have a large polygon and different building activities within that area which produced positive and negative ST-differences from 1991 to 2000. The averaging process has

smoothed these differences so that no change is indicated. Additional problems are given by the high number of mixed pixels. Each pixel represents the mean radiance of surfaces covering a square of ca 15,000 m² (TM 5) or 3,600 m² (TM 7). Therefore no representative ST can be derived for linear features (highways, railroad tracks) and small polygons.

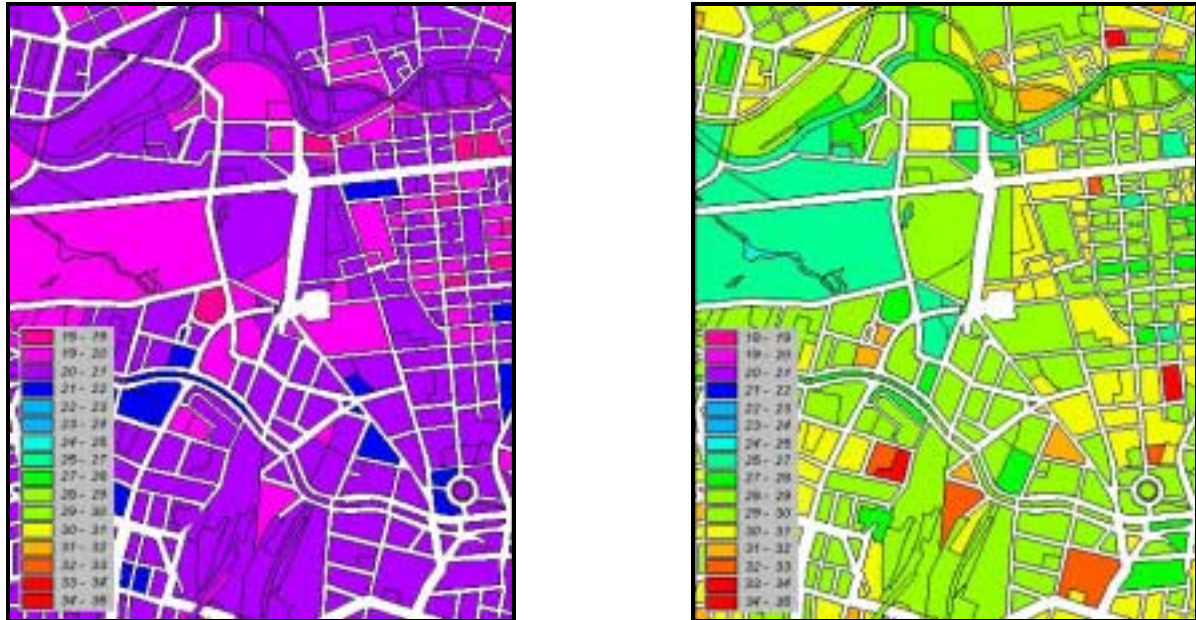


Fig. 3: Surface temperatures related to urban structure polygons, example “Potsdamer Platz”;
 a) night situation 13.08.2000; b) day situation 14.08.2000 (surface temperatures in ° Celsius)



Fig. 4: Day-night-difference of surface temperatures and NDVI related to urban structure polygons, example “Potsdamer Platz”;
 a) day-night-difference 14.08.00/13.08.00 in Kelvin; b) NDVI extracted from ETM+ in DN calculated with following term $((B4-B3)/(B4+B3)+1)*127$

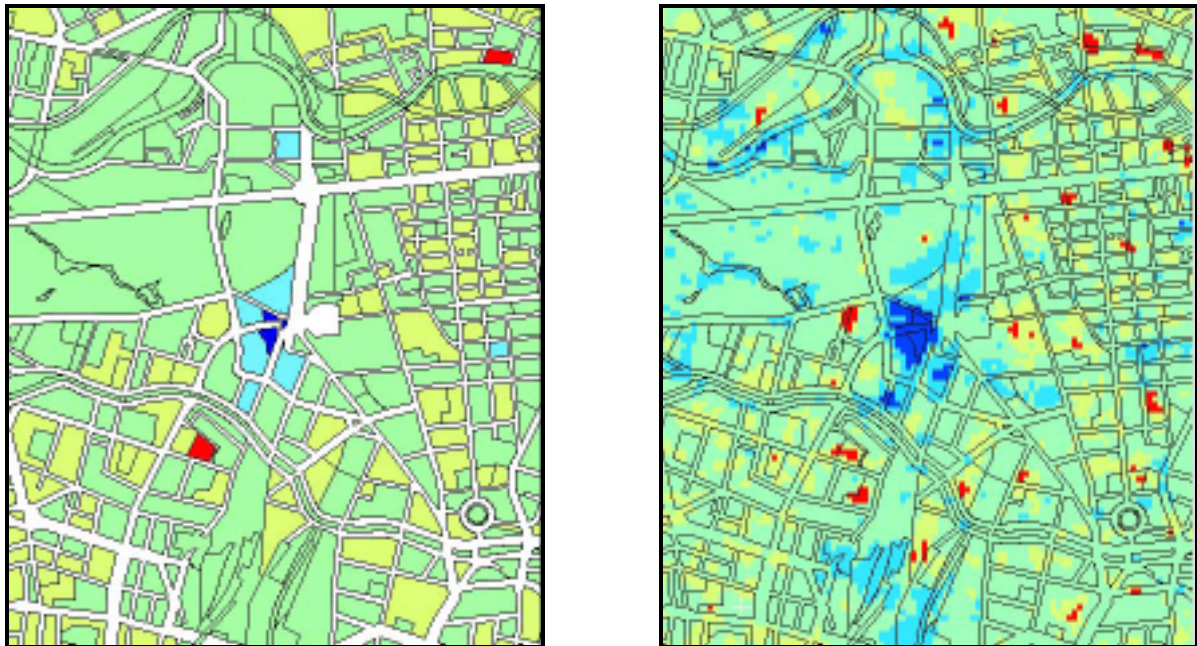


Fig. 5: Comparison of the changes of the day-and-night differences 1991/ 2000 related to the polygons representing the urban structures or related to each satellite pixel – example 1 ‘Potsdamer Platz’ (range form blue – green – red; blue – lower day-night-differences in 2000; red – lower day-night-differences in 1991)

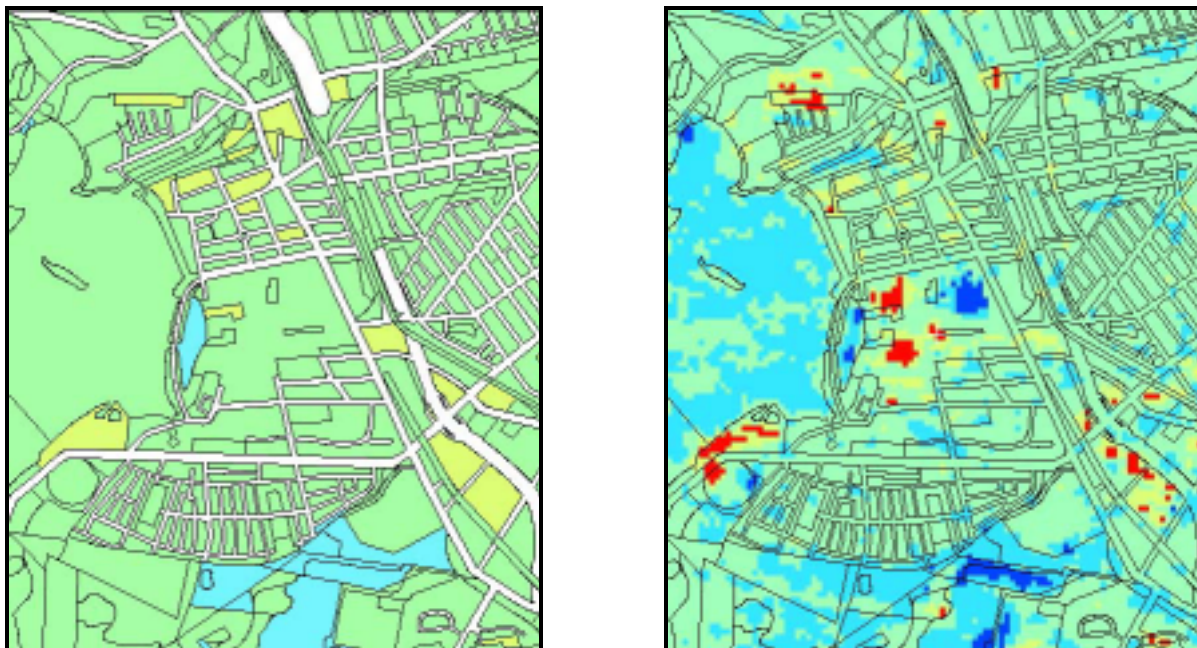


Fig. 6: Comparison of the changes of the day-and-night differences 1991/ 2000 related to the polygons representing the urban structures or related to each satellite pixel – example 2 ‘Tegel’ (range form blue – green – red; blue – lower day-night-differences in 2000; red – lower day-night-differences in 1991)

L_U_KEY	D91MT	D00MT	N91MT	N00MT	DIF91MT	DIF00MT	NDVI91	NDVI00	DD00M91	VG
No_key	21.12	29.55	10.65	18.07	10.43	11.41	158.13	135.39	0.94	16.82
B_site	22.00	30.35	11.98	18.95	9.95	11.39	133.10	114.34	1.44	3.93
C&i	22.40	31.28	12.04	19.43	10.32	11.87	134.43	108.29	1.55	74.10
Camp	18.74	26.78	12.55	19.12	6.22	7.52	168.27	144.08	1.26	15.52
fields1	22.09	30.39	11.63	18.89	10.44	11.51	142.19	121.22	1.06	14.50
fields2	22.63	31.05	9.53	17.13	13.06	13.92	150.74	127.18	0.86	2.10
for_ext	19.60	27.13	11.46	18.66	8.13	8.33	163.87	144.98	0.16	2.06
for_gen	18.79	26.67	11.90	19.22	6.97	7.31	176.80	159.30	0.31	1.21
for_int	19.25	26.63	11.59	18.68	7.70	7.76	169.75	153.59	0.03	2.49
for_mix	20.67	28.90	11.67	19.14	8.98	9.66	163.06	139.00	0.65	6.81
res	20.92	29.54	11.85	19.25	9.04	10.20	151.51	126.91	1.13	38.57
res1	21.56	30.41	12.89	20.04	8.61	10.42	137.14	112.04	1.82	67.05
res2	21.77	30.62	12.28	19.55	9.44	11.11	138.31	112.79	1.68	60.34
res3	20.45	28.72	12.76	19.58	7.76	9.06	149.77	124.84	1.33	57.56
reskern	21.92	30.64	13.35	20.15	8.51	10.53	126.04	99.63	2.04	81.73
se1	21.37	30.04	12.45	19.62	8.90	10.41	144.27	121.14	1.52	55.77
se2	21.78	30.53	12.36	19.55	9.42	11.00	138.42	113.73	1.59	68.21
se_prom	21.40	30.02	12.97	20.23	8.44	9.79	141.39	114.56	1.36	57.71
se_sport	21.14	29.71	12.08	19.08	9.05	10.58	154.41	130.19	1.53	48.12
se_traff	21.68	30.39	12.27	19.68	9.37	10.71	141.90	117.30	1.34	79.34
ve_ag1	19.77	27.88	12.51	19.12	7.28	8.63	165.63	141.09	1.33	23.91
ve_ag2	20.85	29.28	11.57	18.95	9.25	10.21	161.92	136.92	0.95	22.79
ve_cem	20.15	28.29	12.03	19.32	8.16	8.86	166.05	144.53	0.66	16.40
ve_green	21.73	29.69	9.83	17.26	11.85	12.38	160.51	142.72	0.50	2.29
ve_mead	22.39	30.48	10.62	18.05	11.74	12.41	152.29	131.75	0.68	7.81
ve_mix	21.60	29.82	11.43	18.90	10.12	10.87	153.37	131.40	0.76	8.37
ve_nurs	21.23	29.65	11.01	18.36	10.22	11.20	152.51	129.07	0.97	34.46
ve_park	20.49	28.70	12.21	19.47	8.28	9.13	160.41	138.04	0.82	11.59
water	19.89	27.15	12.29	19.64	7.60	7.43	151.69	130.42	-0.20	0.00
global	20.92	29.37	11.89	19.22	9.01	10.08	152.45	129.12	1.05	35.37

Table 4: Mean surface temperatures, mean differences, NDVI and sealing density for all land use types (see Tab. 2 for land use key details).

4.2 CORRELATION BETWEEN NDVI, BUILDING DENSITY AND THERMAL IRRADIANCE

It is well known that the NDVI is negative correlated with surface radiant temperature (LO et al., 1997) and with sealing density (see col. NDVI00 or NDVI91 in Table 3). These correlations can be visualised by plotting the corresponding MST values for all land cover types into scattergrams (Fig. 7). Figure 7b shows that the range of NDVI values for small sealing density almost covers the whole range of the abscissa. The corresponding land cover types (see Table 4) are water, forests, parks and mixed vegetation covers with high NDVI and fields with sparse vegetation or bare soils.

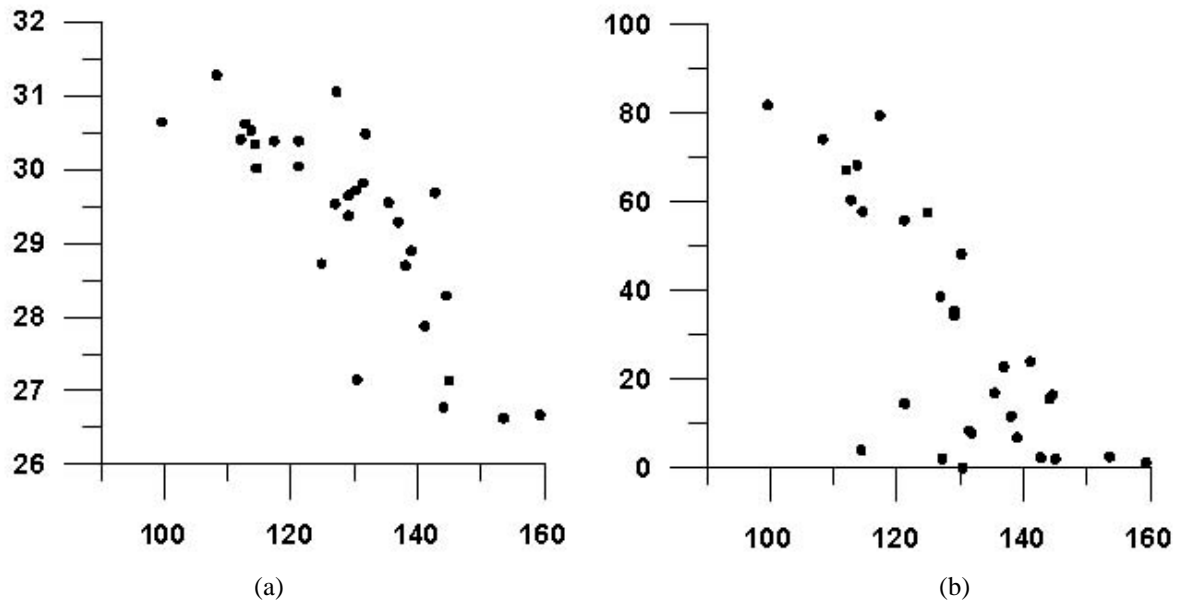


Fig. 7: (a) Scattergram of average daytime surface temperature vs. NDVI ($r=-0.73$) and (b): average NDVI vs. sealing density ($r=-0.72$). The NDVI (abscissa) is calculated by using $NDVI = ((B4-B3)/(B4+B3)+1)*127$.

A scattergram of day-night temperature contrast vs. NDVI (Fig. 8) shows a point pattern which preserves the cluster structure obtained from MSTs of day-night-pairs (see App. 1b): In Fig. 8 water and all forest cover types (group 1) are plotted in the right lower corner of the diagram, a transition zone contains forest intermingled with other urban green spaces (cemeteries, parks and allotment gardens – group 3). Residential areas and service areas (group 4a + b) are located in the centre of the diagram (medium values for both parameters, NDVI and MST contrasts). In other words: the NDVI confirms the cluster structure of land cover types derived from day-night MSTs.

To demonstrate the heterogeneity of land use covers defined in the municipal GIS database a random subset of ca. 100 polygons was selected and their mean values for NDVI and SFT were plotted into corresponding scattergrams (see App. 2 a,b). Residential cover types spread over the whole diagram and even forest polygons exhibit a wide range of NDVI values from 105 to 170 (see bottom row in App. 2b).

5. SUMMARY AND CONCLUSIONS

This study has achieved several research objectives by combining thermal infrared remote sensing data with GIS. The comparison of two pairs of Landsat TM day-night-time scenes in 1991 and 2000 revealed significant changes of land use in the area of Greater Berlin and demonstrated the power and limitations of geometrical and thematic urban structure information used in the municipal GIS. The averaging process of thermal signatures for each urban structure block facilitates the interpretation of the thermal map of the city as well as the evaluation of different land cover types in contributing to the urban climate. But the block size of the urban structure cover is too big for monitoring land use and for detecting land use changes. The statistical analysis of thermal information, sealing density and vegetation indices confirms that each of them contains independent information which should be used for the analysis of urban environment. Cluster analysis of 30 land use types defined in the municipal data base can be applied with different variable sets to create more homogeneous groups with respect to different problems for the urban environment (increasing building density, monitoring of vegetation indices, detection of urban heat islands). These studies on mean block values should be completed by monitoring representative test sites defined with standard image classification procedures based on multi-spectral/multi-temporal pixel information.

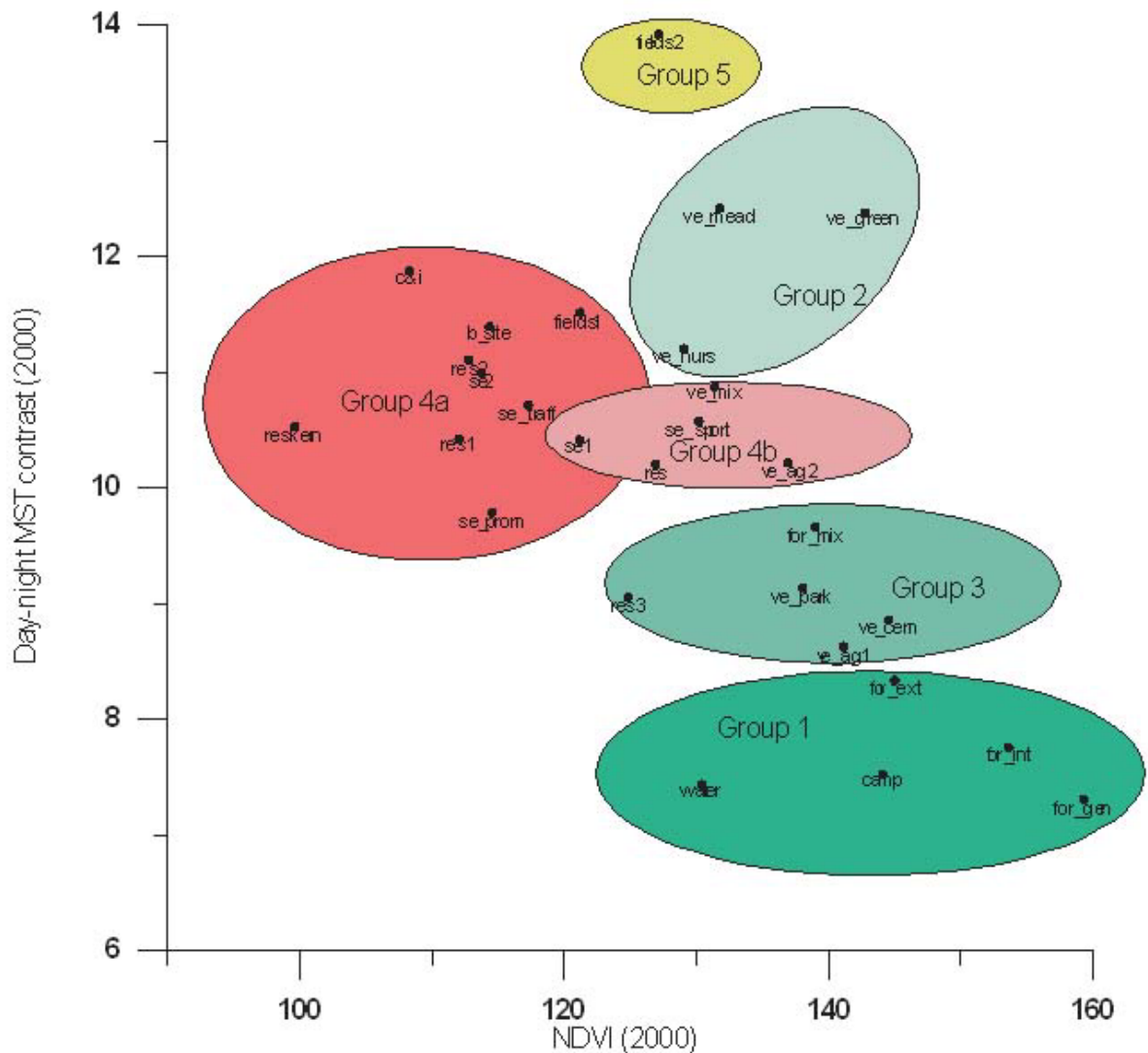


Fig. 8: Scattergram of mean day-night radiance contrast vs. NDVI. Labels indicate land use cover type (see Table 1 for details)

6. ACKNOWLEDGEMENT

We acknowledge the financial support provided by the Senate of Berlin represented by the Senate Department of Urban Development which ordered the Landsat TM scenes and funded image processing and production of thematic maps. We are especially grateful to J. Welsch and T. Schneider who provided us with all necessary information about the urban (municipal) GIS.

7. REFERENCES

- ESA European Space Agency (1984): TM digital product description. - Earthnet Programme Office, Rev.1., 19 S., Fucino.
- LO, C.P., QUATTROCHI, D.A. & J.C. LUVALL (1997): Application of high-resolution thermal infrared remote sensing and GIS to assess the urban heat island effect.- *Int. J. Remote Sensing*, **18**, 287 - 304.
- MARKHAM, B. & BARKER, J. L. (1986): Landsat MSS and TM postcalibration dynamic ranges, exoatmospheric reflectances and at-satellite temperatures. - EOSAT Landsat tech. Notes, 1, p. 3 - 7, Lanham (EOSAT).
- NASA (1982): Landsat Data User Notes. - U.S. Geol. Survey/ NOAA/ Sioux Falls.

NASA (1984): A prospectus for Thematic Mapper research in the Earth Sciences. - NASA Tech. Memo. 86149, 66 pp., Goddard Space Flight Center, Greenbelt.

NASA (2000): Landsat 7 – Science Data Users Handbook. - http://ftpwww.gsfc.nasa.gov/IAS/handbook/handbook_toc.html

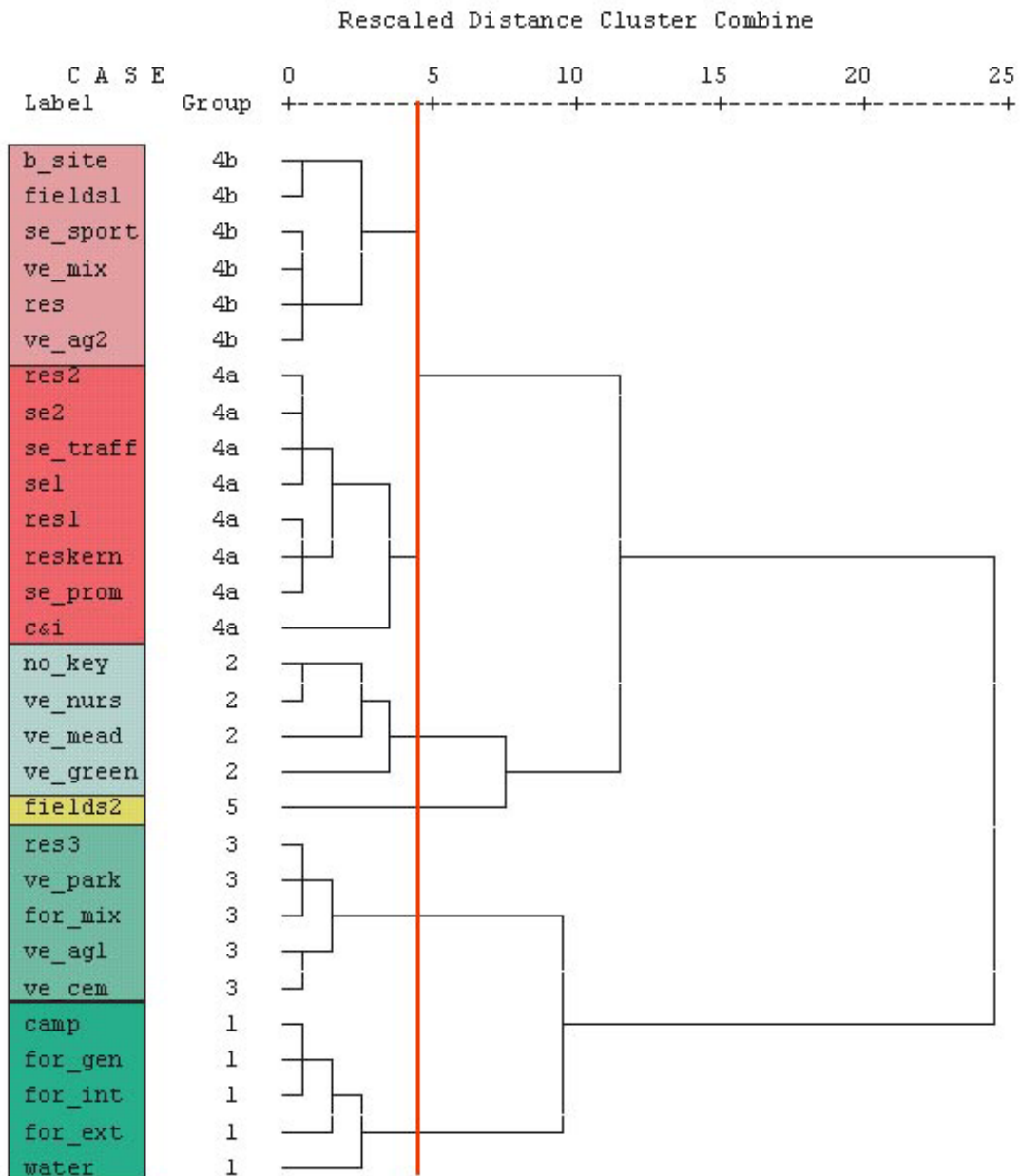
OBENSCHAIN, A., WILLIAMS, D., ANDARY, J. (1998): Landsat 7: Extending the Landsat tradition into the next century. – Space Technol. 18, 1/2, 3-10.

SCHOTT, J.R. & VOLCHOCK, W.J. (1985): Thematic Mapper infrared calibration. - Photogramm. Eng. remote Sens., 51, 9, p. 1351 - 1357, Falls Church, VA.

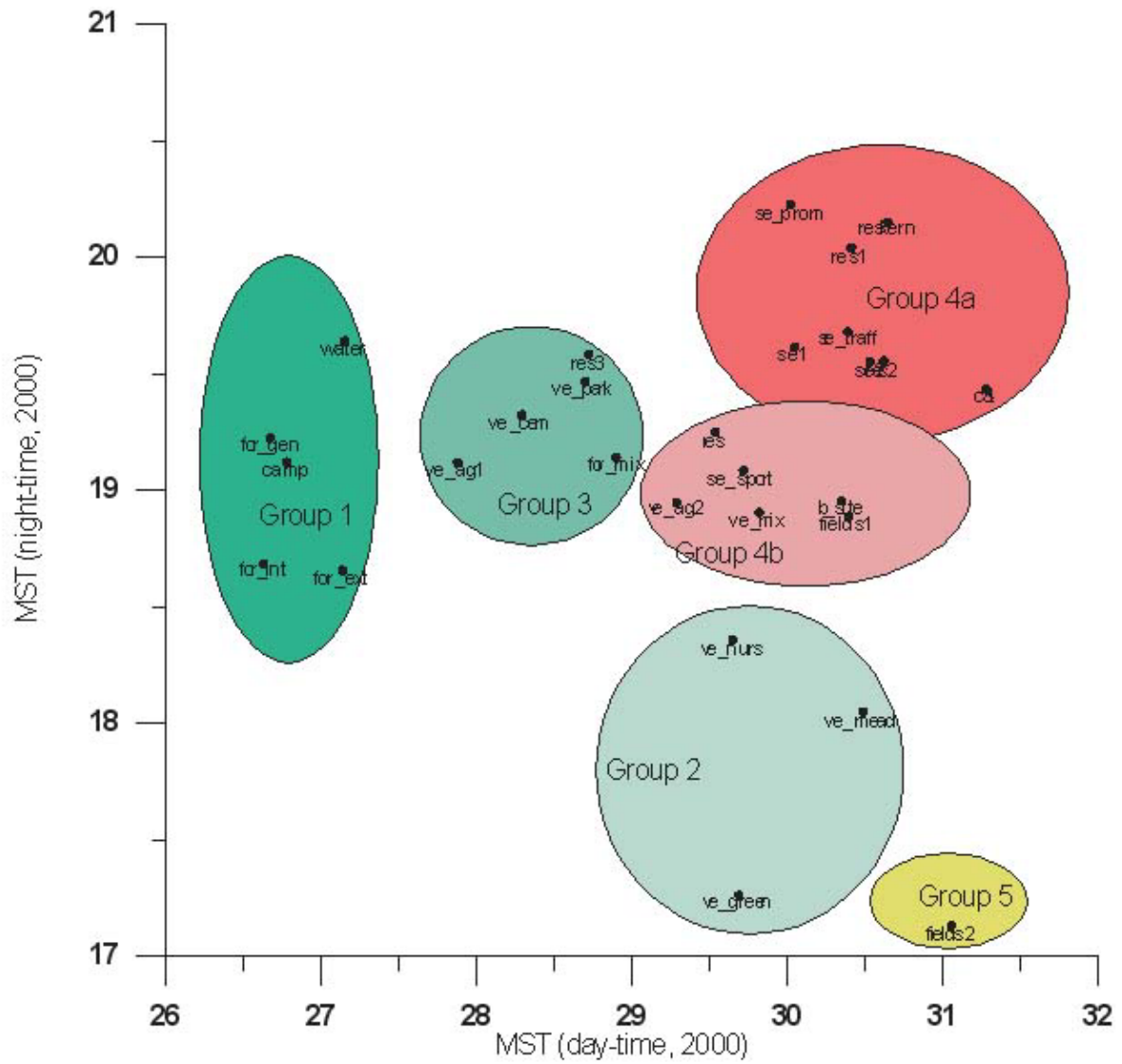
SENATSV ERWALTUNG FÜR STADTENTWICKLUNG (1985): Umweltatlas Berlin (printed edition); see <http://www.stadtentwicklung.berlin.de/umwelt/umweltatlas/> for updated digital edition).

SINGH, S.M. (1988): Brightness temperature algorithms for Landsat Thematic Mapper data. - Remote Sens. Envir., 24, p. 509 - 512, New York, NY.

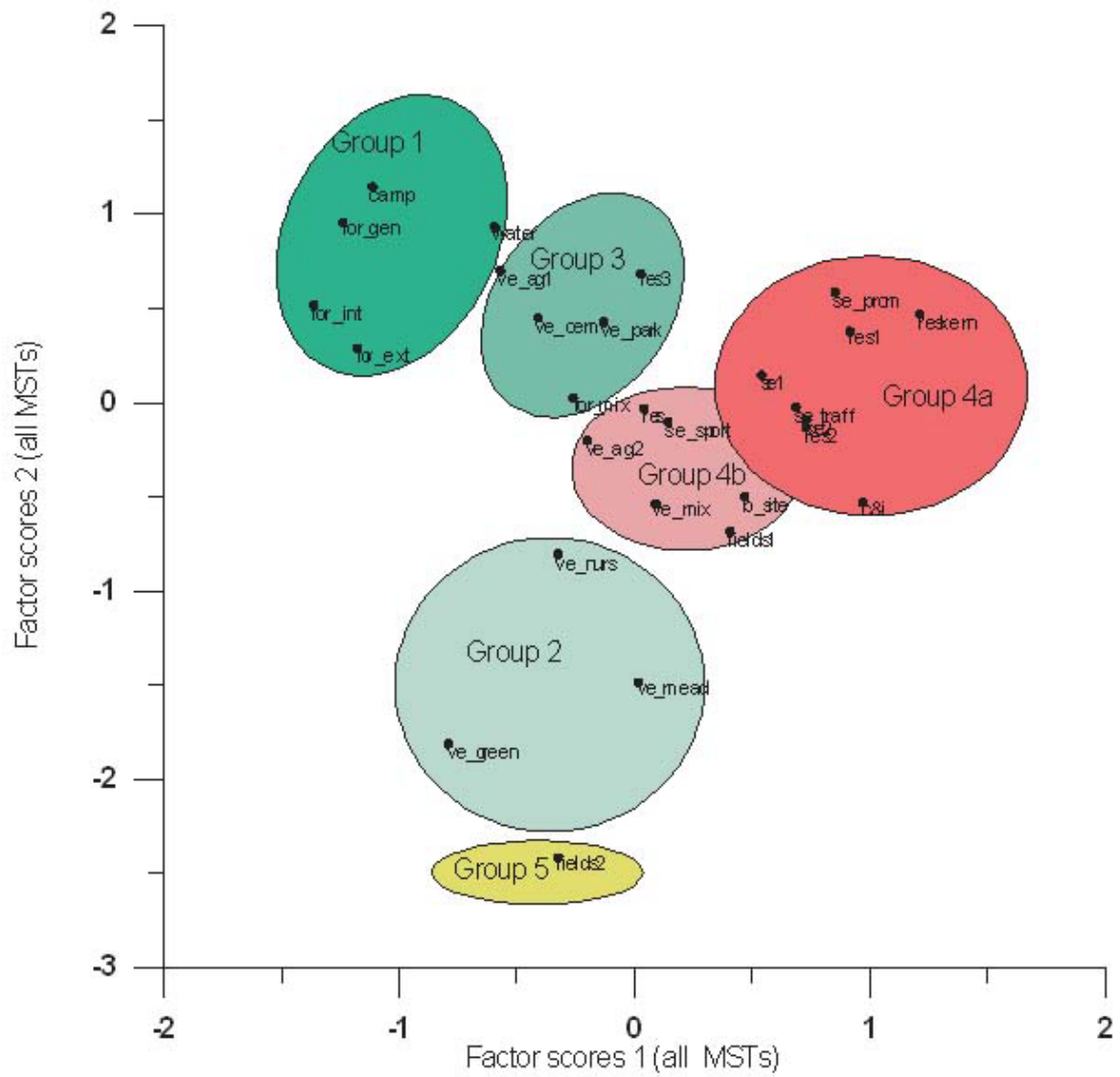
Appendix 1:



App. 1a: Dendrogram of land cover types using average day-night-time surface temperatures

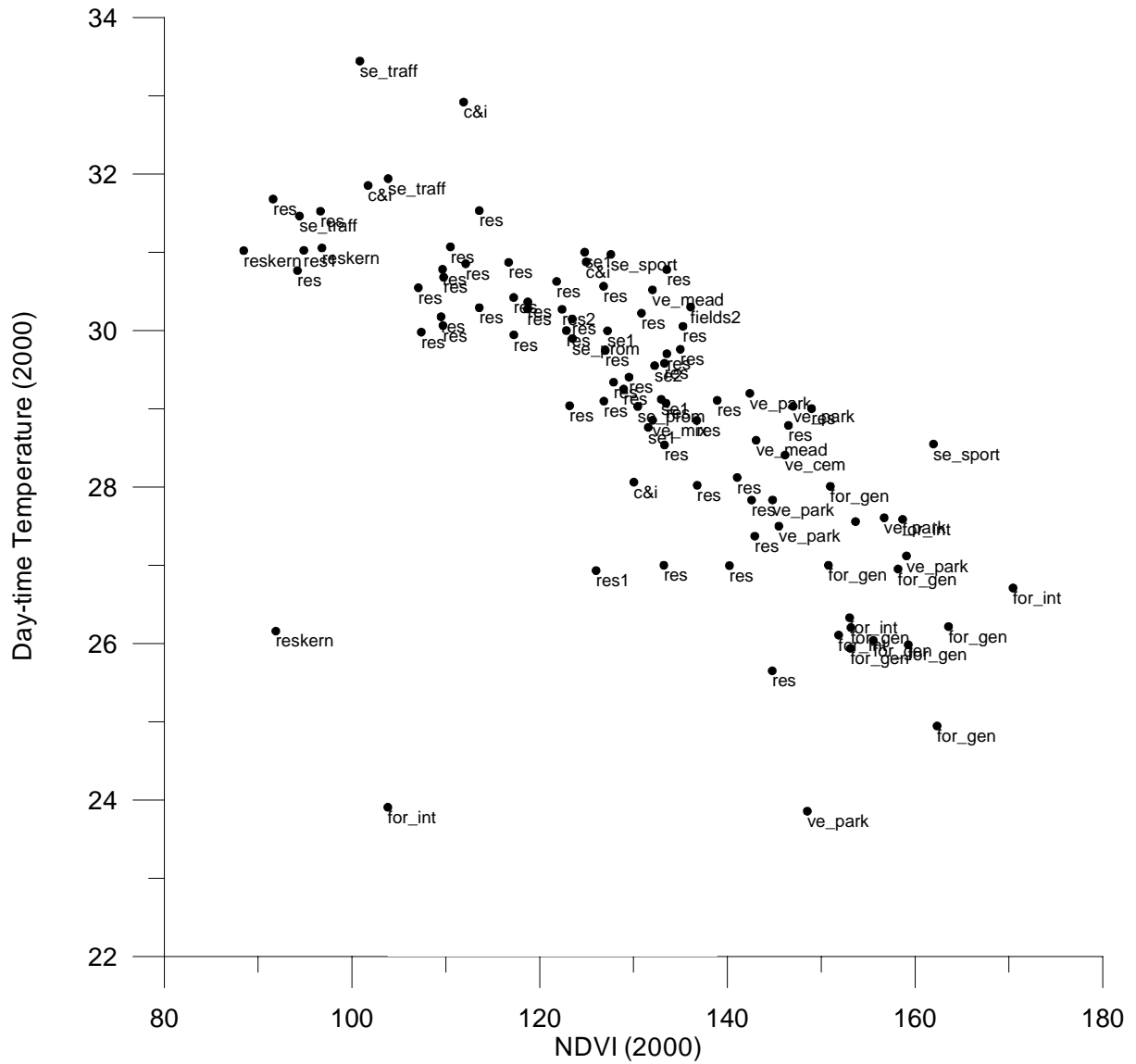


App. 1b: Scattergram of land cover types using average day-night-time surface temperatures

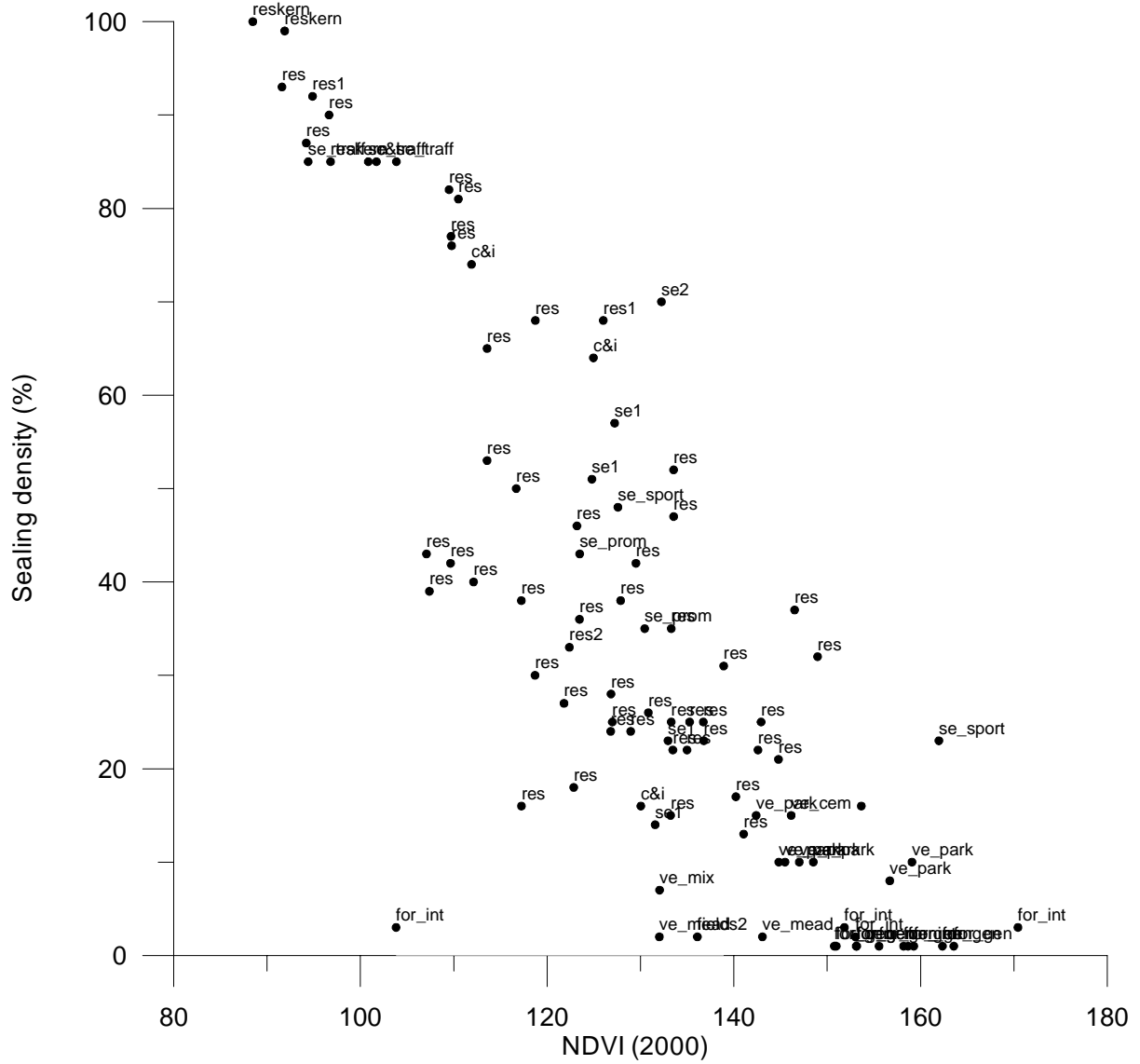


App. 1c: Scattergram of factor scores for two factors extracted from 1991 and 2000 day-night-time mean surface temperatures

Appendix 2



App. 2a: Scattergram of NDVI vs. daytime temperature values for 96 random polygons (labels see Table 1).



App. 2b: Scattergram of NDVI vs. sealing density shows high variability within land use cover types (labels see Table 1).